*Published online 18 January 2017*

*Nucleic Acids Research, 2017, Vol. 45, No. 6* ***3231–3241***
*doi: 10.1093/nar/gkx001*

# Self-cytoplasmic DNA upregulates the mutator enzyme APOBEC3A leading to chromosomal DNA damage

**Rodolphe Suspène[1], Bianka Mussil[1,2], Hélène Laude[1], Vincent Caval[1], Noémie Berry[1], Mohamed S. Bouzidi[1], Valérie Thiers[1], Simon Wain-Hobson[1] and Jean-Pierre Vartanian[1,*]**

[1]Molecular Retrovirology Unit, Institut Pasteur, 28 rue du Dr. Roux, 75724 Paris cedex 15, France and [2]Unit of Infection Models, German Primate Centre, Kellnerweg 4, 37077 Goettingen, Germany

Received August 20, 2016; Revised December 29, 2016; Editorial Decision December 29, 2016; Accepted January 02, 2017

## ABSTRACT

**Foreign and self-cytoplasmic DNA are recognized by numerous DNA sensor molecules leading to the production of type I interferons. Such DNA agonists should be degraded otherwise cells would be chronically stressed. Most human APOBEC3 cytidine deaminases can initiate catabolism of cytoplasmic mitochondrial DNA. Using the human myeloid cell line THP-1 with an interferon inducible *APOBEC3A* gene, we show that cytoplasmic DNA triggers interferon α and β production through the RNA polymerase III transcription/RIG-I pathway leading to massive upregulation of *APOBEC3A*. By catalyzing C→U editing in single stranded DNA fragments, the enzyme prevents them from re-annealing so attenuating the danger signal. The price to pay is chromosomal DNA damage in the form of CG→TA mutations and double stranded DNA breaks which, in the context of chronic inflammation, could drive cells down the path toward cancer.**

## INTRODUCTION

The *APOBEC3* (*A3*) locus consists of seven genes (*A3A-A3C, A3DE, A3F-A3H*) (A3) on chromosome 22 that encodes DNA cytidine deaminases (1). These enzymes preferentially deaminate single strand DNA (ssDNA), leading to a huge number of CG→TA transitions especially in the context of 5′TpC and 5′CpC dinucleotides (2–5). The cellular location of the A3A enzyme is both cytoplasmic and nuclear while A3B is exclusively nuclear (6,7). Despite this, A3A is the more active of the two enzymes (6,8,9). Their role in cancer is highlighted by the fact that many cancer genomes encode tens of thousands of C→T transitions frequently in the 5′TpC dinucleotide context, a hallmark of A3A and A3B cytidine deamination (10–12).

Epidemiological studies have shown that a 29.5 kb *A3B* deletion polymorphism, whereby all but the last exon of *A3B* is deleted, is correlated with a higher odds ratio of developing breast, ovarian and HBV-associated liver cancer (13,14). Breast cancer genomes from $\Delta A3B^{-/-}$ patients harbor a higher mutation burden (15) while the chimeric *A3A* transcript resulting from the *A3B* deletion leads to greater intracellular steady state levels of A3A (6). In so doing, these studies indicate that *A3A* alone can generate human cancers, and show that the $\Delta A3B$ lesion is a causal cancer susceptibility marker (6,15).

Cancer emerges on a background of chronic inflammation (16), HBV, HCV, HPV, KSHV, HTLV-1, Merkel cell polyomavirus or *Helicobacter pylori* being well-known etiological agents. TLR9 recognizes CpG DNA resulting in IFNα (Interferon) production in plasmacytoid dendritic cells (17). Intracellular DNA can be captured by a myriad of DNA sensor molecules leading to the triggering of potent innate immune responses (18). The cytosolic DNA binding protein LRRFIP1 interacts with β-catenin and promotes its activation by phosphorylation (19). After binding to the C-terminal domain of the transcription factor IRF-3, IFNβ production is initiated (19). Recently, it was shown that the intracellular sensor cGAS can detect cytoplasmic DNA and induce type I IFN responses (20). Equally, AT-rich DNA can trigger type I IFN responses via intracytoplasmic transcription of double stranded DNA (dsDNA) by RNA polymerase III to form dsRNA intermediates that are sensed by RIG-I (21,22). Interestingly, these different pathways have in common STING (STimulator of INterferon Gene) that was shown to be pivotal for the production of type I IFNs (23). STING itself interacts with both MAVS and RIG-I, themselves crucial to interferon signaling (24).

As mitochondrial DNA fragments (mtDNA) resemble bacterial DNA in possessing unmethylated CpG motifs, they too can trigger cytoplasmic DNA sensor molecules leading to inflammatory responses (25). Mitochondrial

*To whom correspondence should be addressed. Tel: +33 1 44 38 94 45; Fax: +33 1 45 68 88 74; Email: jean-pierre.vartanian@pasteur.fr
Present address: Bianka Mussil, Unit of Infection Models, German Primate Centre, Kellnerweg 4, 37077 Goettingen, Germany.

DNA can induce TLR9-mediated inflammatory responses in cardiomyocytes and is even capable of inducing myocarditis (26). Cellular disruption and necrosis can release mtDNA into the circulation causing systemic inflammation (27), while extracellular DNA can be taken up into endosomes and sensed by specific TLRs (17).

Despite the wealth of knowledge concerning cytoplasmic DNA signaling, there is much less data on the fate of the DNA agonist, for the danger signal has to be countered, otherwise cells would be chronically stressed. This is suggested by the fact that germ line mutations in some endo- and exonuclease genes result in symptoms resembling chronic inflammation (28,29). Cytoplasmic mitochondrial DNA is deaminated by any of the six functional APOBEC3 enzymes. *A3A* and *A3G* are of special note as they are upregulated by IFNα (4,30–32), by contrast, A3B is not. As the highly efficient enzyme uracil N-glycosylase and abasic pyrimidine/purine endonucleases mobilize around A3A edited DNA, the three enzymes effectively function as a cytidine specific endonuclease reducing ssDNA to very small fragments.

It is shown here for the human monocytic cell line THP-1, that transfected dsDNA is sensed and transcribed by RNA polymerase III leading to dsRNA intermediates that were captured by RIG-I ultimately leading to type I interferon production. In turn A3 cytidine deaminases were induced, particularly A3A which resulted in deamination and catabolism of the transfected DNA agonist. The data highlight the A3 cytidine deaminases as anti-inflammatory agents. The sting in the tail is A3A mediated chromosomal DNA damage.

## MATRIALS AND METHODS

### Reagents

dUTP was from Sigma, RNA polymerase III inhibitor (ML-60218) was from Merck Millipore, dNTP (Fermentas), type I IFNα were from PBL Biomedical Laboratories, CpG (Invitrogen), polyIC and peptidoglycan (from *Staphylococcus aureus*, InvivoGen), Taq Polymerase (BIOTAQ DNA polymerase, Bioline), Pfu (Agilent Technologies), cGAS siRNA (sc-95512), pol III RPC39 siRNA (sc-36292), pol III RPC62 siRNA (sc-76188) were from Santa Cruz Biotechnology, STING (antibody #3337), phospho-IRF-3 (Ser396) (4D4G, rabbit mAb #4947), IRF-3 (D6I4C, XP rabbit mAb #11904), β-catenin antibody (amino-terminal antigen, #9581), mouse anti-rabbit IgG (conformation specific, L27A9, mAb #3678), anti-rabbit IgG, HRP-linked (antibody #7074), cGAS (D1D3G, mAb#15102) antibodies were from Cell Signaling Technology. APOBEC3A antibody (SAB4500753) was from Sigma Aldrich. RIG-I (E-5, sc-376882), pol III RPC39 (C 39-2, sc-23913), pol III RPC62 (I-18, sc-69534) antibodies were from Santa Cruz Biotechnology, Inc. Anti-mouse IgG, (HRP-linked antibody #NA931V) was from GE Healthcare. Monoclonal anti-β-actin−peroxidase (antibody #A3854) was from Sigma Aldrich. Human IFNα (IgA, mba-hifnα-3), hIFNβ (IgG, mbg-hifnβ-3), hIFNγ (IgA, mba-hifnγ-3) and Mouse IgG2a (mbg2a-ctrlm) antibodies used as control were from InVivogen.

### Cell culture and transfection

THP-1 cells (ATCC® TIB-202™) were maintained in RPMI (Eurobio), supplemented with 50 U/ml penicillin and 50 μg/ml streptomycin, and 10% heat-inactivated fetal calf serum. Cells were grown in 75 $cm^2$ cell culture flasks at 37°C in a humidified atmosphere containing 5% $CO_2$. For transfection $1.5 \times 10^6$ THP-1 cells were seeded in 12-well tissue culture plates and incubated for 24 h. DNA transfections were performed using jetPRIME (Polyplus transfection reagent). At 24 h post-transfection, supernatants were harvested and IFNα (VeriKine™ Human IFN Alpha Multi-subtype ELISA Kit) and IFNβ (VeriKine™ Human IFN Beta Multi-subtype ELISA Kit) were quantified and analyzed (PBL Assay Science). All DNAs were extracted using the MasterPure Complete DNA and RNA purification kit (Epicentre Biotechnologies).

$2 \times 10^5$ THP-1 cells were plated in 6-well tissue culture plate in 1 ml antibiotic-free growth medium supplemented with fetal bovine serum (FBS). Cells were transfected according to standard protocol (Santa Cruz Biotechnology) with siRNA specific for RNA pol $III_1$ (sc-76188) and RNA pol $III_2$ (sc-36292), for cGAS (sc-95512) and control siRNA (sc-37007), using siRNA transfection reagent (sc-29528) and siRNA transfection medium (sc-36868). Six hours post-transfection with siRNA, cells were transfected with 500 ng of *MT-COI* DNA using jetPRIME. At 24 h, RNA was extracted, cDNA synthesized and A3A expression quantified by real time polymerase chain reaction (PCR). Data were normalized to the expression levels of the housekeeping reference gene *RPL13A*.

Approximately $1.5 \times 10^6$ THP-1 cells were transfected using jetPRIME (Polyplus transfection reagent) with 500 ng of *MT-COI* DNA in quintuplicate. At 24 h post-transfection supernatants were grouped together and clarified by centrifugation. One ml of supernatant was incubated with 2 μg or 10 μg/ml of antibody against IFNα, or IFNβ, or IFNγ for 1 h and added to $1.5 \times 10^6$ fresh THP-1 cells. At 24 h RNA was extracted, cDNA synthetized and A3A expression quantified by real time PCR. Data were normalized to the expression levels of the housekeeping reference gene *RPL13A*. THP-1 cells were transfected using jetPRIME (Polyplus transfection reagent) with 500 ng of *MT-COI* DNA or *V1V2* DNA. Two hours post-transfection, cells were incubated with RNA polymerase III inhibitor (ML-60218) and were collected 22 h post-incubation. Total RNA was extracted, cDNA synthetized and A3A expression quantified by real time PCR. Data were normalized to the expression levels of the housekeeping reference gene *RPL13A*.

### FACS analysis for DNA double stranded breaks

Twenty-four hours post-transfection, THP-1 cells were washed with PBS, fixed in 2% ice-cold paraformaldehyde (Electron Microscopy Sciences) for 15 min and permeabilized in 90% ice-cold methanol (Sigma) for 30 min. After two washes with PBS, cells were incubated for 1 h with 1:100 diluted Alexa Fluor 488-conjugated mouse monoclonal anti-γH2AX (N1-431) antibody (BD Pharmingen). All incubation steps were performed on ice. Cells were analyzed on MACSQuant Analyzer (Miltenyi Biotec) using

the MACsQuantify™ Software (Miltenyi Biotec) or FlowJo software (Tree Star, Inc., version 8.7.1). For each sample 10 000 cells were counted.

### PCR/3DPCR

For amplification of human *MT-CYB*, the first-round reaction parameters were 95°C for 5 min, followed by 40 cycles (95°C for 30 s, 60°C for 30 s and 72°C for 2 min) and finally 10 min at 72°C. Second round 3DPCR were performed using the equivalent of 1 μl of the first round reaction as input. For second-round 3DPCR, the reaction parameters were 75–85°C for 5 min, followed by 40 cycles (75–85°C for 30 s, 60°C for 30 s and 72°C for 2 min) and finally 10 min at 72°C. All amplifications were carried out using 2.5 U Taq (Bioline) DNA polymerase per reaction. *MT-COI* DNA (511 bp) and *inMT-COI* DNA (247 bp) corresponding to the mitochondrial cytochrome oxidase gene were amplified. PCR conditions and primers were described before (4,33). HIV-1 V1V2 region amplification was already described (34). Upon migration on agarose gel (1.5%), PCR products were purified using Nucleospin Gel and PCR clean-up Kit (Macherey-Nagel), $inMT\text{-}COI_{0\ mut.}$ (*inMT-COI* DNA without mutation) and $inMT\text{-}COI_{32\ mut.}$ (*inMT-COI* DNA with 32 G→A mutations) were selected among the hypermutated *inMT-COI* DNA library.

### Real-time PCR and SYBR Green quantitative PCR

Total RNA was extracted from THP-1 cells using RNeasy Plus Mini Kit (Qiagen) according to the manufacturer's instructions. Synthesis of cDNA was performed with 1 μg RNA using the Quantitec Reverse Transcription Kit (Qiagen). Quantitative PCR was performed using cDNA samples and TaqMan Universal PCR Master Mix (Applied Biosystems) for human A3A to A3H. Primers and PCR condition were described before (35). Data were normalized to the expression levels of the housekeeping reference gene *RPL13A*. For the real-time PCR based on SYBR Green, quantitative PCR was performed using DNA samples. Conditions were 10 min at 95°C then 20 s at 95°C, 20 s at 55°C and 2 min at 68°C for 40 cycles.

### Western blotting

Total protein was recovered 24 h post-transfection from cells in a lysis buffer (20 mM Tris–HCl pH 7.5, 150 mM NaCl, 1 mM $Na_2EDTA$, 1 mM EGTA, 1% Triton, 2.5 mM sodium pyrophosphate, 1 mM beta-glycerophosphate, 1 mM $Na_3VO_4$, 1 μg/ml leupeptin) (Cell Signaling, #9803) in presence of protease inhibitor (Roche). Gels used were NuPAGE 4–12% Bis-Tris Gel (Invitrogen). Western blot analysis was carried out according to standard procedures by using a mouse or rabbit monoclonal specific antibodies. The immunoassay used a membrane made of nitrocellulose (GE Healthcare Life science). After incubation with an anti-mouse IgG horseradish peroxydase-coupled secondary antibody (Amersham), the membrane was subjected to detection by enhanced chemiluminescence (Pierce). β-Actin was used as a loading control using 1/25000 diluted mouse monoclonal antibody specific for β-actin (Sigma Aldrich).

### RNA protein co-immunoprecipitation and RT-PCR

Eight hours post-transfection of 500 ng of HIV-1 *V1V2* DNA, $1.5 \times 10^6$ THP-1 transfected cells were incubated with 37% formaldehyde (to a final concentration of 1%) for 15 min at room temperature under gentle shaking. Cross-linking was stopped by adding 2 M glycine to a final concentration of 0.2 M for 5 min at room temperature. Cells were then centrifuged at 1800 *g* for 5 min at 4°C and lysed in cell lysis buffer (#9803, Cell Signaling) containing 40 U/ml RNasin on ice for 5 min. Lysates were then sonicated on ice three times for 5 s each. After centrifugation at 14 000 *g* for 10 min at 4°C, supernatants were transferred to new tubes and incubated for 1 h at 4°C with 30 μl of 50% protein A agarose bead (#9863, Cell Signaling) under rotation. After 10 min centrifugation at 14 000 *g* and 4°C, supernatants were transferred to fresh tubes and incubated with 20 μl of anti-RIG-I antibody (200 μg/ml) under gentle shaking overnight at 4°C. Thirty microliters of protein A agarose beads were then added and incubated for 30 min at 4°C. After centrifugation at 14 000 *g* for 10 min at 4°C, pellets were washed five times with 500 μl of 1× cell lysis buffer (20 mM Tris–HCl pH 7.5, 150 mM NaCl, 1 mM $Na_2EDTA$, 1 mM EGTA, 1% Triton, 2.5 mM sodium pyrophosphate, 14 mM beta-glycerophosphate, 1 mM $Na_3VO_4$, 1 μg/ml leupeptin) (Cell Signaling, #9803) containing 40 U/ml RNasin. Pellets were resuspended with 50 μl of water and heated to 95°C for 2 min. After centrifugation for 10 min at 4°C, 14 000 *g* RT-PCR was performed on the supernatant.

## RESULTS

### Transfected *MT-COI* DNA upregulates type I interferon and leads to A3A expression

THP-1 is an IFNα-inducible human acute monocytic leukemia cell line that is one of the very few where all *A3* genes are either expressed or can be induced, notably *A3A*. THP-1 cells were transfected by DNA amplified by PCR, corresponding to the mitochondrial cytochrome oxidase gene (*MT-COI*, 511 bp). Supernatants were clarified 24 h post-transfection and IFNα and IFNβ production measured by ELISA. As can be seen in Figure 1A, 500 ng generated strong IFNα and β responses compared to the jetPRIME control. THP-1 cells incubated with 500 ng of *MT-COI* DNA (*MT-COI*),* but not transfected, failed to induce IFNα or IFNβ, indicating that intracellular DNA constitutes the trigger. As THP-1 cells are insensitive to unmethylated CpG and polyIC, IFN induction is not via TLR3 and TLR9 pathways (Figure 1A) (36). A transcription study of APOBEC3 genes showed that $MT\text{-}COI_T$ DNA increased *A3A, A3F, A3G* and *A3H* expression at 24 h in a dose-dependent manner, even at concentrations that did not induce detectable IFNα or IFNβ levels in culture supernatants (Figure 1B). *A3A* was by far the most sensitive to transfected DNA being upregulated by almost four orders of magnitude and confirmed by western blot (Figure 1C) showing the presence of the two A3A isoforms (p1 and p2) (37,38). By contrast, *A3F*, *A3G* and *A3H* were upregulated at most 10-fold (Figure 1B).

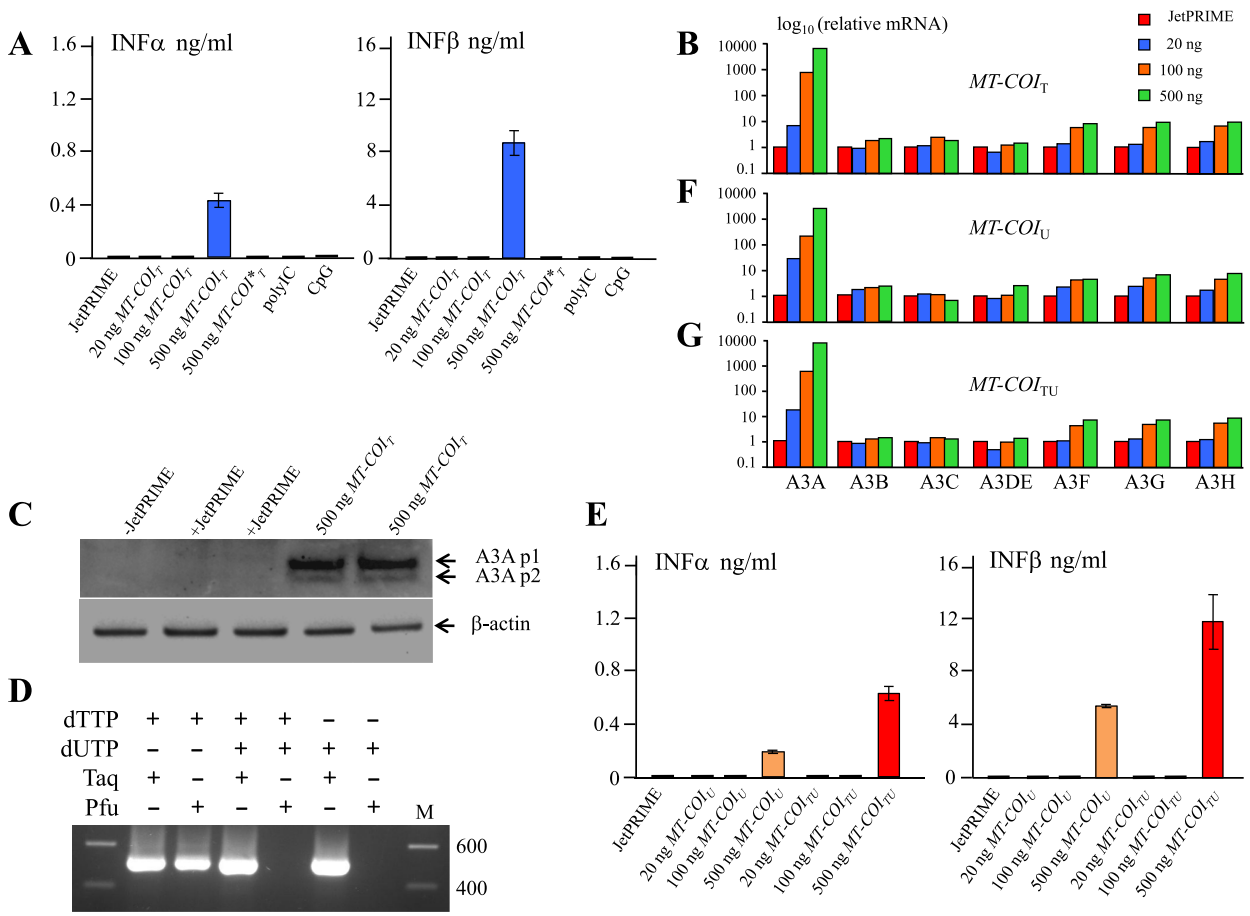


**Figure 1.** Transfected *MT-COI* DNA upregulates type I interferon and A3A expression. (**A**) Interferon α and β production following transfection of THP-1 cells by dT containing PCR DNA fragments. *MT-COI** indicates incubation with DNA but no transfection. (**B**) *APOBEC3* transcription profiling of transfected THP-1 cells. Data were normalized to the expression levels of *RPL13A* housekeeping reference gene. Profiling was performed in duplicate and normalized to JetPRIME to facilitate comparison. (**C**) Western blot of A3A isoforms p1 and p2 from transfected THP-1 and compared to β-actin. Lanes 2, 3 and lanes 4, 5 represent duplicates. (**D**) Agarose gel of *MT-COI* PCR products (511 bp) amplified with *Taq* or *Pfu* polymerase in the presence of dTTP, dUTP, dTTP+dUTP. M, molecular weight markers. (**E**) Interferon α and β production following transfection of THP-1 cells by dU or 50:50 mixture dT+dU containing PCR DNA fragments. (**F** and **G**) Transcriptomes were established for DNA containing dU (F) or a 50:50 mixture of dT and dU (G). Duplicates were normalized to the expression levels of *RPL13A* housekeeping gene and normalized to JetPRIME to facilitate comparison.

### Uracil in cytosolic DNA is not a danger signal

Given that hyperedited cytoplasmic mitochondrial DNA (cymtDNA) bears non-canonical uridine residues, they might constitute a novel danger signal. To explore this hypothesis, *MT-COI* DNA was amplified using either dUTP, an equimolar mix of dTTP and dUTP or just dTTP. To control for the incorporation of dUTP in the DNA, a second round of PCR was performed with internal primers and *Pfu* or *Taq* DNA polymerase. Like all archaeal DNA polymerases, *Pfu* is unable to amplify DNA templates bearing dU (39). As expected *Pfu* PCR failed to recover DNA when dUTP (*MT-COI*$_U$) or mixed nucleotides dUTP+dTTP (*MT-COI*$_{UT}$) were incorporated, in contrast to *Taq* PCR (Figure 1D). When transfected into THP-1 cells both *MT-COI*$_U$ and *MT-COI*$_{UT}$ DNA resulted in induction of IFNα and IFNβ in culture supernatants (Figure 1E) and upregulation of the *A3A, A3F, A3G* and *A3H* genes (Figure 1F and G), although, once again, A3A was upregulated by approximately four orders of magnitude. These data indicate that uracil in DNA does not constitute a novel danger signal.

### Interferon β exerts a paracrine effect on APOBEC3A expression

In order to demonstrate that upregulation of *A3A* by several logs (Figure 1B, F and G) could be amplified by paracrine IFNα/β induction via IFNAR (IFNα/β receptor), THP-1 cells were transfected with 500 ng of *MT-COI*$_T$ DNA. At 24 h post-transfection after clarification, cell supernatant was incubated with 2 or 10 μg/ml of antibody against IFNα or IFNβ or IFNγ and added to 1.5 × $10^6$ fresh THP-1 cells for 24 h. Interestingly, we observed that relative A3A expression was reduced in a dose-dependent manner by one–two orders of magnitude when the supernatant was incubated with anti-IFNβ antibodies (Figure 2A). This experiment suggests that A3A expression could be amplified by the paracrine effect of IFNβ.

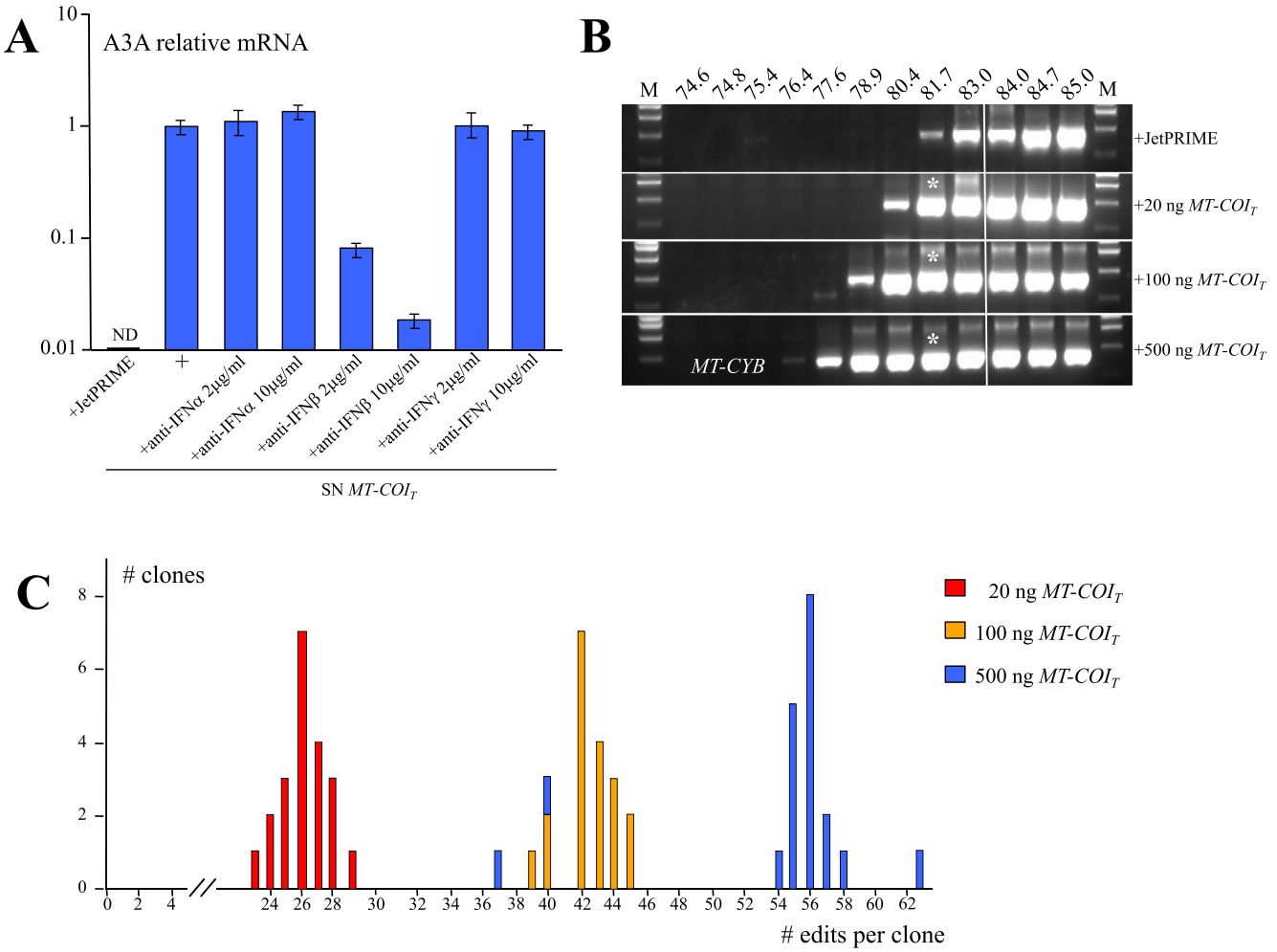


**Figure 2.** Paracrine effect of interferon β and editing of endogenous *MT-CYB*. (**A**) *A3A* relative expression was amplified by paracrine IFNβ induction in THP-1 cells and analyzed with only JetPRIME or transfected with 500 ng of *MT-COI*$_T$ DNA. Cell supernatant (SN-*MT-COI*$_T$) was incubated with 2 or 10 μg of antibody against IFNα, IFNβ or IFNγ for 1 h and added to 1.5 × $10^6$ fresh THP-1 cells for 24 h. ND, not detectable. (**B**) THP-1 DNA transfection increases A3-editing of endogenous cytoplasmic *MT-CYB* DNA recovered by 3DPCR. The white line indicates the threshold between edited and unedited 3DPCR products. Asterisks refer to the samples cloned and sequenced. M: molecular weight markers. (**C**) Frequency distribution of C→T editing per clone as a function of the quantity of DNA transfected.

We have previously shown that transfected DNA amplified by PCR can be deaminated by endogenous A3 enzymes (34). In order to see if the induction of *A3* genes by exogenous DNA could result in editing of endogenous cymtDNA, THP-1 cells were transfected with *MT-COI*$_T$ DNA and analyzed at 24 h. Cytochrome b mtDNA (*MT-CYB*) was amplified by 3DPCR as previously described (4). 3DPCR recovered DNA at denaturation temperatures lower than for the jetPRIME control, indicative of increased A3 editing (Figure 2B). 3DPCR products recovered at 81.7°C were cloned and sequenced. The sequences were peppered by C→T substitutions, the mean editing frequency per sequence increasing with the quantity of transfected DNA (Figure 2C).

## Cytosolic dsDNA induces APOBEC3A leading to double-stranded DNA breaks

In order to distinguish whether ssDNA or dsDNA was the IFN agonist, four pairs of complementary oligonucleotides corresponding to a small region of *MT-COI* were synthesized, $WT_{1+2}$ (43 bp, 51% GC) and $WT_{3+4}$ (39 bp, 56% GC) while oligos $Hyp_{1+2}$ (43 bp, 7% GC) and $Hyp_{3+4}$ (39 bp, 13% GC) correspond to hypermutated forms of $WT_{1+2}$ and $WT_{3+4}$ respectively (Supplementary Table S1). THP-1 cells were transfected with DNA duplexes and IFNα induction measured (Figure 3A). $WT_{1+2}$ and $WT_{3+4}$ (dsDNA) were potent inducers of IFNα, and on a par with the 511 bp *MT-COI* DNA fragment, whereas the mismatched pairs of oligos, $WT_{1+3}$ or $WT_{2+4}$, effectively ssDNA, failed to induce IFNα (Figure 3A). As the complementary oligonucleotides $Hyp_{1+2}$ and $Hyp_{3+4}$ did not induce IFN expression, it is probable that they did not form stable heteroduplexes at 37°C given their low GC content, only 7–13%.

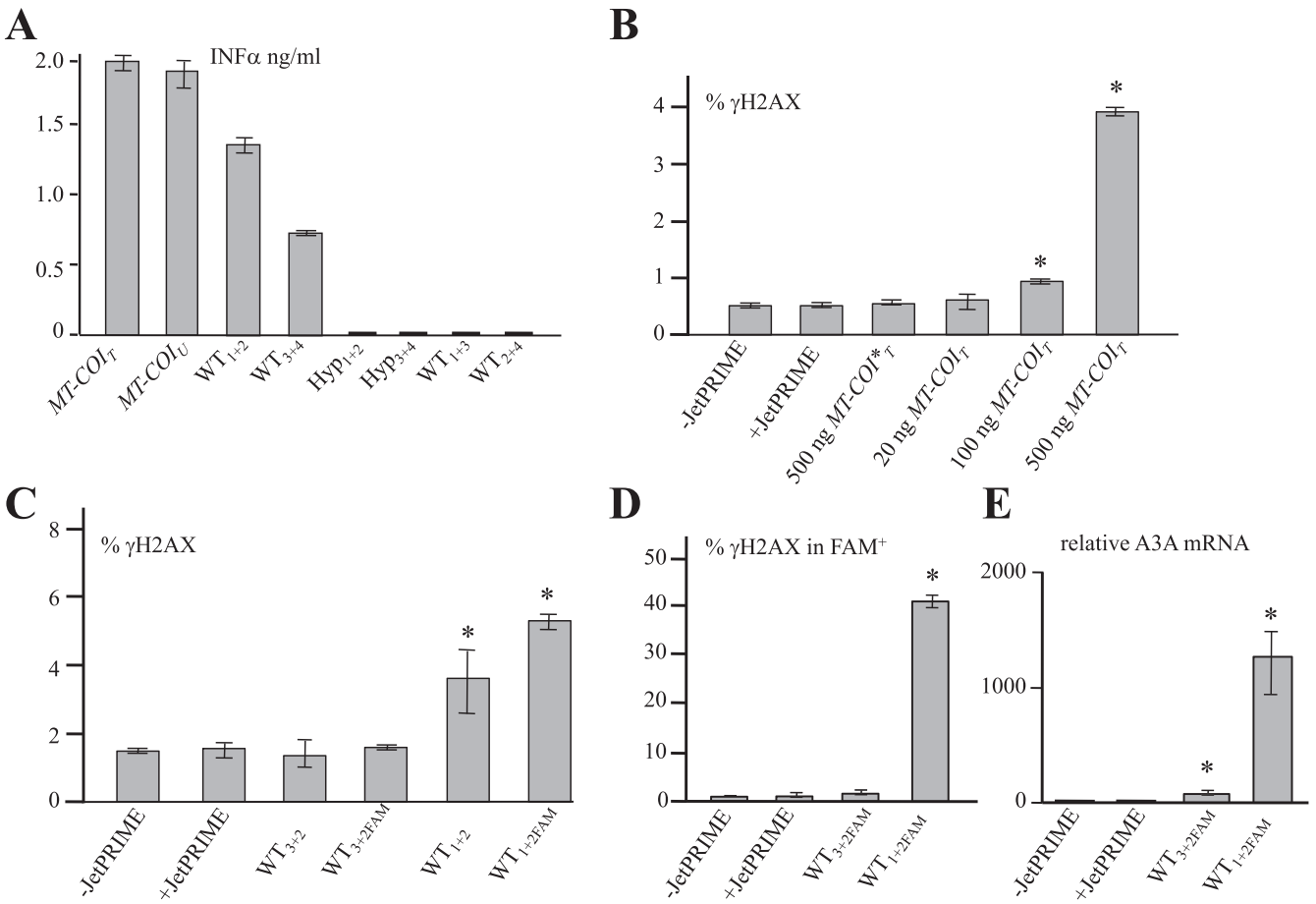


**Figure 3.** Transfected *MT-COI* DNA induces double-stranded DNA breaks. (**A**) Interferon α production following transfection of THP-1 cells by 500 ng $MT\text{-}COI_T$ or $MT\text{-}COI_U$, 500 ng of $WT_{1+2}$, $WT_{2+3}$, $Hyp_{1+2}$, $Hyp_{3+4}$, $WT_{1+3}$ and $WT_{2+4}$ (Supplementary Table S1). (**B**) FACS analysis of γH2AX-positive THP-1 cells transfected with *MT-COI*. Means and standard deviation of γH2AX-positive cell frequencies for duplicate transfection. (**C**) FACS analysis of γH2AX-positive DSBs in THP-1 transfected with $WT_{3+2}$, $WT_{3+2FAM}$, $WT_{1+2}$ and $W_{1+2FAM}$ respectively. Means and standard deviation of γH2AX-positive cell frequencies for duplicate transfection. (**D**) FACS analysis of γH2AX-positive DSBs in THP-1 transfected with cells gated on FAM-positive cells after transfection with $WT_{3+2FAM}$ and $W_{1+2FAM}$ respectively. Means and standard deviation of γH2AX-positive cell frequencies for duplicate transfection. (**E**) Transcription profiling of A3A in THP-1 transfected cells with $WT_{1+2FAM}$ (dsDNA) or $WT_{3+2FAM}$ (ssDNA) respectively, in presence or absence of JetPRIME. '*' indicates statistically significant difference between two observed percentages ($P < 0.05$, Student's *t*-test).

*MT-COI* DNA transfection of THP-1 cells led to significantly increased DSBs (Figure 3B) as expected from *A3A* upregulation (Figure 1B). To focus on the transfected cells alone, THP-1 cells were transfected with pairs of oligonucleotides one being labeled with the Fluorescein (FAM)-fluorophore i.e. $WT_{1+2FAM}$ (dsDNA) or $WT_{3+2FAM}$ (ssDNA). Twenty-four hours post-transfection, addition of FAM to the DNA oligos did not induce DSBs ($WT_{3+2}$ versus $WT_{3+2FAM}$ and $WT_{1+2}$ versus $WT_{1+2FAM}$, Figure 3C). However, as FAM-fluorescence decreased over time, FAM+ positive cells were sorted 6 h post-transfection, cultured for a further 18 h and fixed for DSB FACS analysis. $WT_{1+2FAM}$ led to ∼40% of γH2AX positive THP-1 cells (Figure 3D) which was correlated with *A3A* upregulation (Figure 3E).

### Cytosolic dsDNA is transcribed by RNA polymerase III impacting RIG-I

Which of the cytosolic dsDNA sensing pathway is upstream of IFN induction? At 24 h post-transfection of THP-1 cells by *MT-COI* DNA, western blot analysis showed increased levels of the phosphorylated forms of TBK1 (TBK1-P) and IRF3 (IRF3-P) as well as DNA dependent increases in RIG-I and MDA5 (Figure 4A). Steady state levels of STING, IKKε, MAVS were unchanged. Dose dependent increases of TBK1-P and IRF3-P, key regulators of IFN production, suggest signaling via STING and/or MAVS. As the RNA polymerase III and cGAS DNA sensor molecules are upstream of STING we explored these possibilities.

As RNA polymerase III has been implicated in the transcription of cytosolic dsDNA (21,22), THP-1 cells were transfected with $MT\text{-}COI_T$ or $MT\text{-}COI_U$ DNA along with ML-60218, an inhibitor of RNA polymerase III (40) (Figure 4B). There was an inverse correlation between IFNα production and inhibitor concentration. To exclude drug toxicity, 20 μg/ml of peptidoglycans (PGN) known to stimulate IFNα via TLR2, was used with ML-60218. IFN production was insensitive to all inhibitor concentrations used (Figure 4B). The inhibitor abolished transfected $MT\text{-}COI_T$

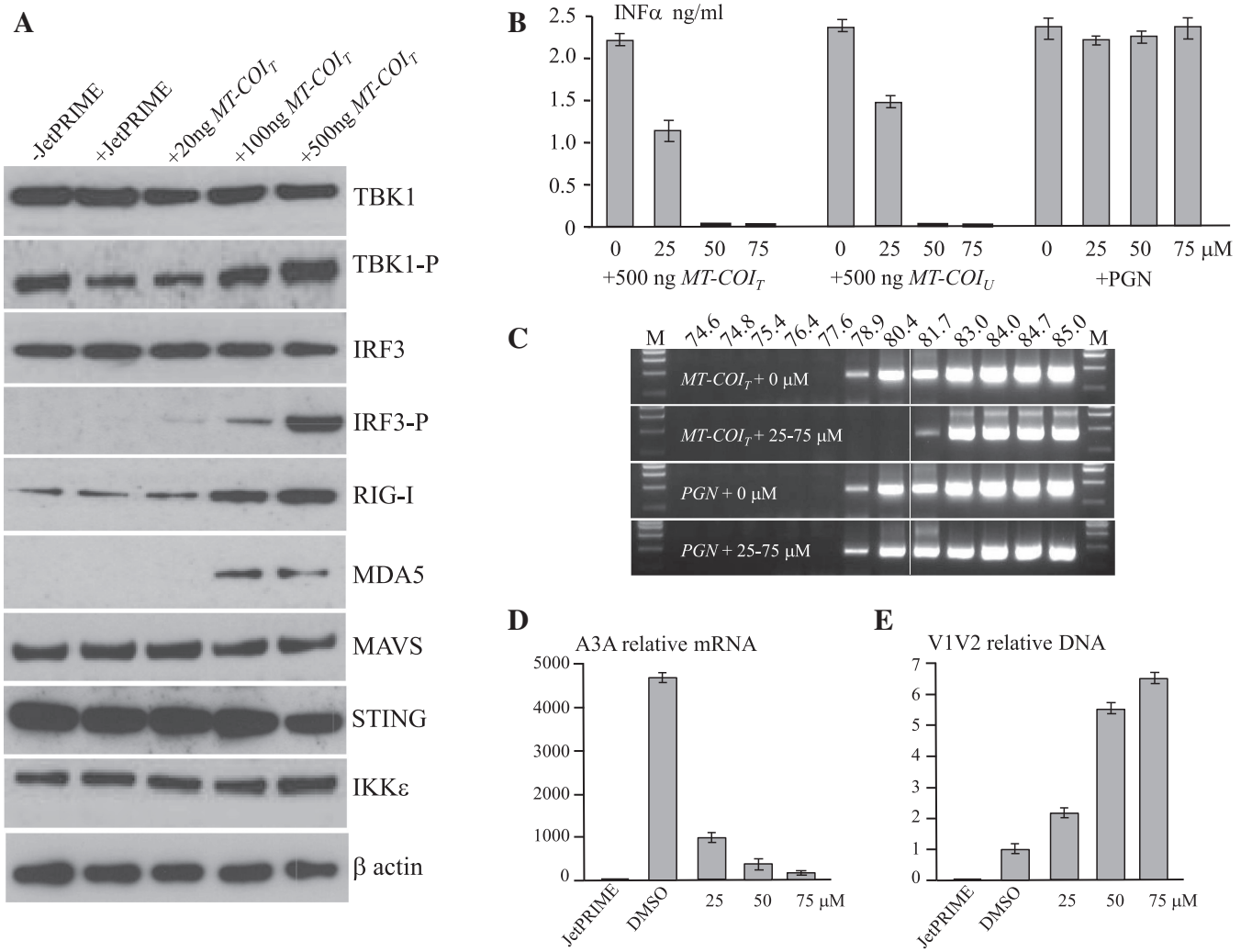


**Figure 4.** Transfected dsDNA triggers the RIG-I pathway via RNA polymerase III. (**A**) Western blots of TBK1, TBK1-P (phosphorylated), IRF3, IRF3-P (phosphorylated), RIG-I, MDA5, MAVS, STING, IKKε at 24 h post DNA transfection of THP-1 cells. (**B**) Interferon alpha production by DNA transfected THP-1 cells along with RNA Polymerase III inhibitor (ML-60218). Peptidoglycans (PGN) were used as control. (**C**) A3-edited *MT-CYB* DNA recovered by 3DPCR in presence or absence of 25–75 µM of RNA polymerase III inhibitor. The white line indicates the threshold between edited and unedited 3DPCR products. M: molecular weight markers. (**D** and **E**) Transcription profiling of A3A and quantification of *V1V2* DNA upon *V1V2* DNA transfected THP-1 cells along with RNA polymerase III inhibitor (ML-60218).

DNA induced A3 mediated hyperediting of endogenous cytoplasmic *MT-CYB* DNA (Figure 4C versus Figure 2B), again something that treatment with PGN and ML-60218 alone or in combination failed to do (Figure 4C).

To correlate RNA polymerase III activity with A3A expression, 500 ng of *V1V2* DNA were transfected in THP1 cells. Two hours post-transfection, cells were incubated with different amounts of RNA polymerase III inhibitor (25, 50 or 75 µM, or DMSO used as negative control). The level of A3A mRNA was quantified by TaqMan PCR (Figure 4D) and *V1V2* DNA by SYBR Green (Figure 4E). The increase of *V1V2* quantification was inversely proportional to the relative A3A expression. This experiment demonstrated that A3A expression could not be detected when RNA polymerase III activity was inhibited (Figure 4D) leading to maintain *V1V2* DNA (Figure 4E).

To confirm the implication of RNA polymerase III in the transcription of cytosolic dsDNA knockdown experiments were performed using siRNAs to each of the subunit transcripts notably pol $III_1$ and pol $III_2$. When compared to control siRNA in THP-1 cells, the two RNA polymerase III siRNAs knockdown restricted A3A relative expression by ∼4–5-fold (Figure 5A). Efficiency of cGAS, and RNA polymerases III siRNAs were confirmed by western blotting (Figure 5B). When cGAS siRNA were used, we observed a slight decrease of A3A expression but remained similar to control siRNA (Figure 5A), suggesting that in THP-1 cells, cGAS played a minor role in interferon type I production.

If cymtDNA was signaling via the RIG-I pathway downstream of RNA polymerase III, it should be possible to identify the pol III RNA transcripts. In the previous experiments a strong background would come from endogenous mtRNA transcripts. To overcome this, THP-1 cells were transfected by PCR products corresponding to a segment of HIV-1 envelope (V1V2, 685 bp, 38% GC (34)). THP-1 cells transfected with 500 ng of *V1V2* DNA in-

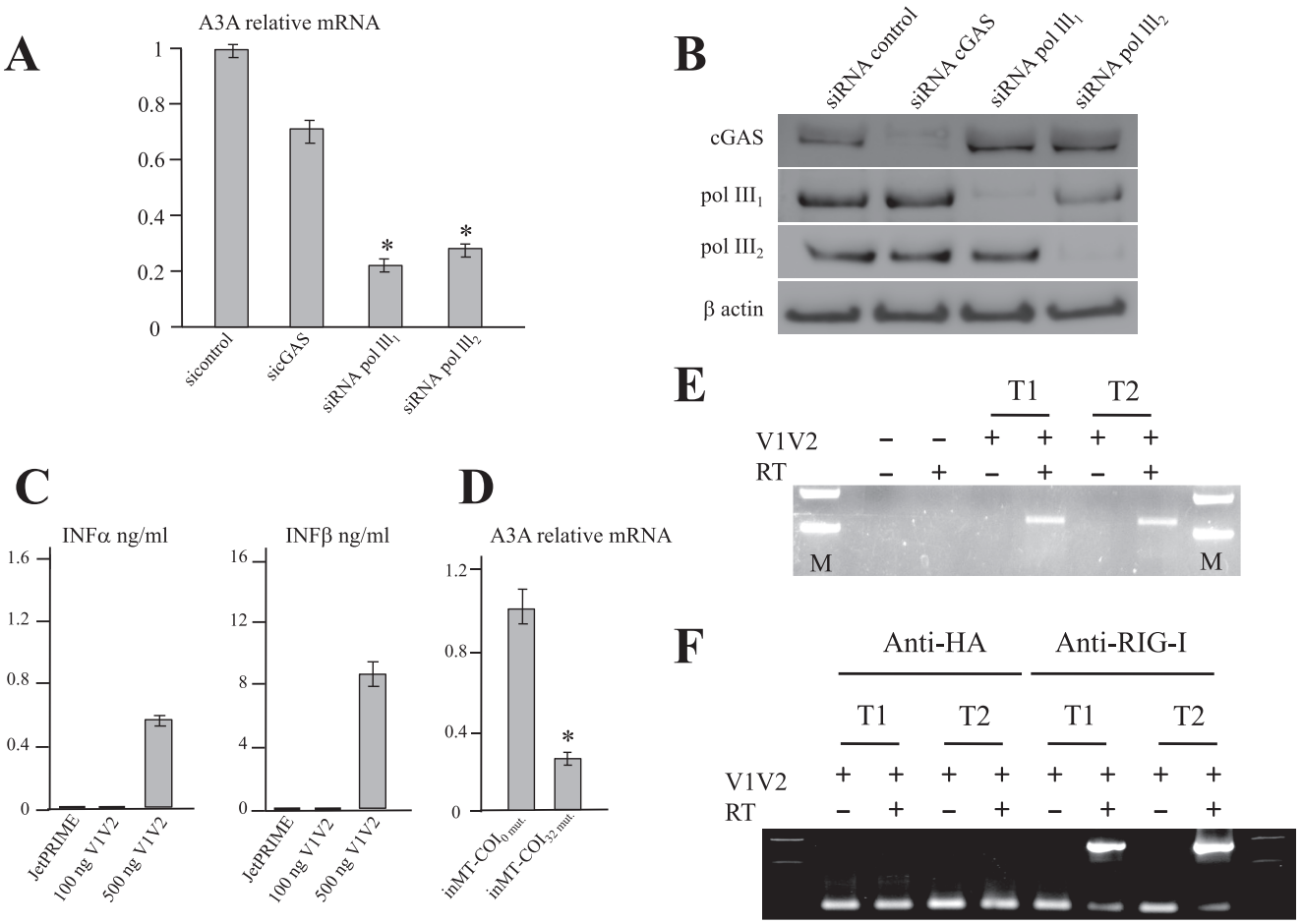


**Figure 5.** Cytoplasmic RNA synthesis by DNA-dependent RNA polymerase III binds to RIG-I. (**A**) THP-1 cells were transfected with control siRNA or 2 RNA polymerase III siRNA (siRNA polIII$_1$ and siRNA polIII$_2$) or cGAS siRNA. Six hours post-transfection with siRNA, cells were transfecte with 500 ng of *MT-COI* DNA. At 24 h post-transfection, total RNA was extracted and quantitative PCR was performed on A3A. (**B**) WB control of the experiment performed in 5A, using cGAS, pol III$_1$ and pol III$_2$ antibodies. The β-actin loading controls are shown below. (**C**) Interferon alpha and beta production by THP-1 following transfection by 500 ng *V1V2* HIV-1 DNA. JetPRIME was used as control. (**D**) A3A quantification by THP-1 following transfection by 500 ng *inMT-COI*$_{0\ mut.}$ and *inMT-COI*$_{32\ mut.}$ DNA. (**E**) V1V2 RNA transcripts from DNA transfected THP-1 cells. Total RNA was extracted at 24 h and a cDNA corresponding to V1V2 was produced in presence or absence of RT and amplified by PCR. T1 and T2 refer to independent transfections. (**F**) Immunoprecipitation with an anti-RIG-I monoclonal antibody performed at 8 h along with an anti-HA as control. V1V2 specific RT-PCR products were recovered only from anti-RIG-I immunoprecipitation. RT, T1 and T2 as for 5E. '*' indicates statistically significant difference between two observed values ($P < 0.05$, Student's *t*-test).

duced IFNα/β to a degree comparable to *MT-COI*$_T$ (Figure 5C versus Figure 1A). When comparing a shorter region of *MT-COI* DNA, (*inMT-COI* DNA, 247 bp, 50% GC), *inMT-COI*$_{0\ mut.}$ (*inMT-COI* DNA without mutation) to *inMT-COI*$_{32\ mut.}$ (*inMT-COI* DNA with 32 mutations, 37% GC), it transpires that transfected dsDNA needed to be thermodynamically stable to detect A3A expression (Figure 5D).

To show that cytoplasmic RNA synthesis by DNA-dependent RNA polymerase III binds to RIG-I, total RNA was extracted from two independent transfections (T1 and T2), treated with DNase and RT-PCR performed. V1V2 RNA intermediates were recovered only when a reverse transcriptase step was performed (Figure 5E). Cell lysates were made and immunoprecipitation with an anti-RIG-I monoclonal antibody was performed along with an anti-HA as control. V1V2 specific RT-PCR products were recovered only from the anti-RIG-I immunoprecipitates (Figure 5F).

## DISCUSSION

The findings highlight a mechanism by which cytoplasmic DNA induces IFNα/β which in turn induced A3A expression leading to catabolism of the DNA agonist. Cytoplasmic DNA can be exogenous or mtDNA presumably released from a stressed mitochondrial network (41). Double-stranded DNA serves as a template for cytoplasmic RNA synthesis by DNA-dependent RNA polymerase III. The complementary strands anneal to yield dsRNA that is recognized by RIG-I, leading to phosphorylation of IRF3 by TBK1, which upon dimerization and translocation to the nucleus, activates transcription of IFN genes. Interferon in turns activates several *A3* genes leading to heightened

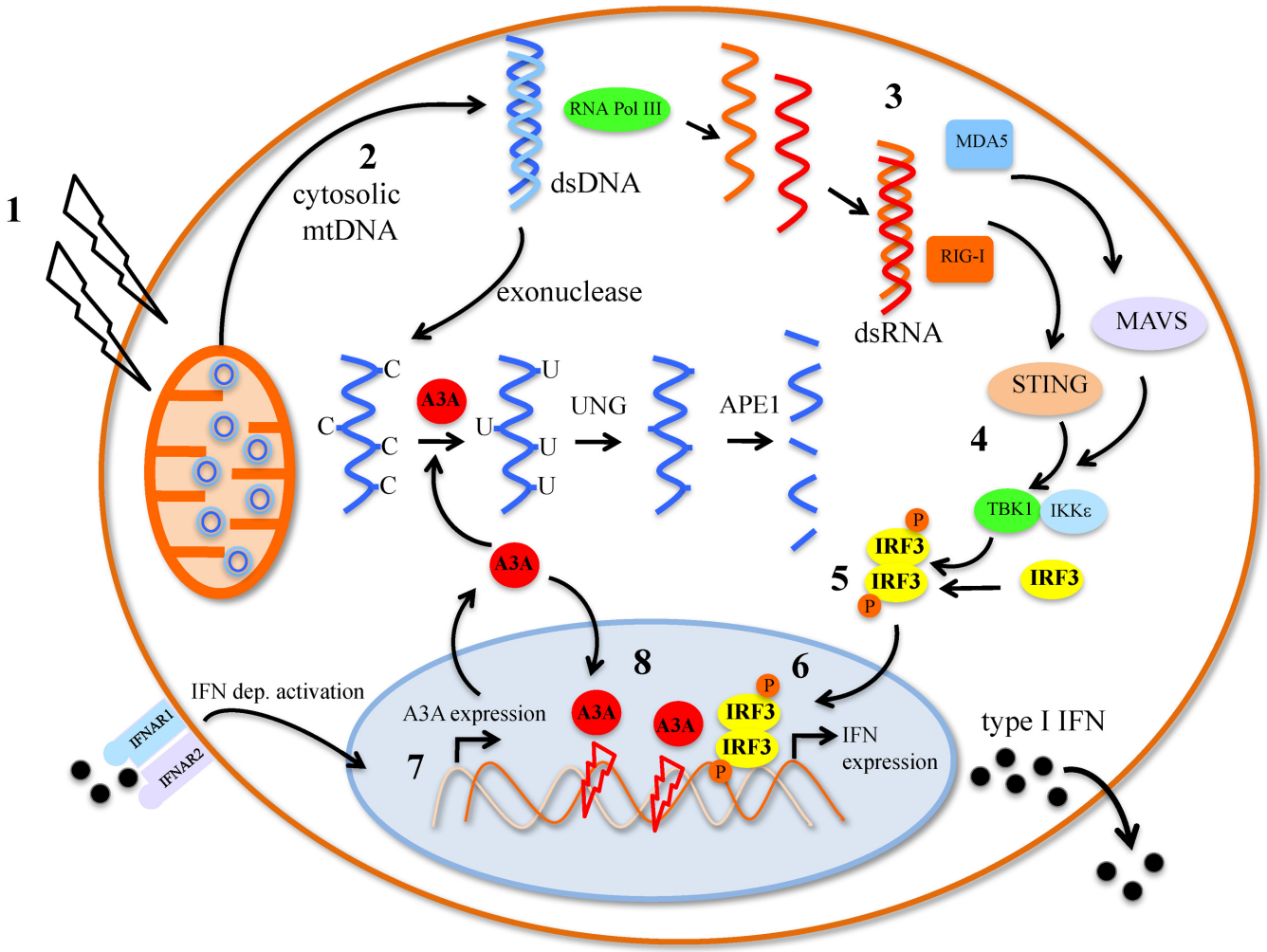


**Figure 6.** Cytosolic DNA mediated innate immune signaling. Upon cellular stress (1), mtDNA is released into the cytoplasm (2) is recognized by RNA polymerase III and transcribed into RNA which anneals to form dsRNA duplexes (3). These activate RIG-I signaling leading to IRF-3 phosphorylated by TBK1 (4-5) and induction of interferon (6). Through IFNAR1/2, signaling IFN production leads to A3A upregulation (7), which initiates catabolism of cytoplasmic ssDNA. As A3A can translocate to the nucleus, it can cause hypermutation of nuDNA and formation of double stranded DNA breaks DSB (8).

catabolism of single stranded DNA generated by cytoplasmic exonucleases (Figure 6).

DNA heteroduplexes as small as 39 bp can be transcribed for IFNα/β induction is almost as efficient as for the 511 bp *MT-COI* fragment (Figure 3A). By comparison, single stranded DNA signaling was weak (Figure 3A). These findings do not exclude other DNA signaling pathways in primary cells for THP-1 cells do not mount TLR3- and TLR9-dependent responses. However, as the ML-60218 inhibitor (Figure 4B, D and E) and RNA polymerase III siRNAs knockdown (Figure 5A) completely blocks IFNα/β induction and A3A expression, RNA polymerase III is the major DNA sensing pathway following transfection of THP-1 cells.

Although A3 enzymes catalyze oxidation of cytidine to uracil in ssDNA, the uracil bases do not constitute a novel danger signal *per se* (Figure 1F, G and E). However, as AU-rich edited DNA is thermodynamically less stable, it represents a mechanism to prevent annealing of complementary ssDNA fragments (Figures 3A and 5D). This is particularly relevant for cymtDNA. If hundreds of mtDNA genomes can leak out to the cytoplasm and be processed by dsDNA-dependent endonucleases and exonucleases, there is the possibility that complementary single stranded mtDNA molecules could re-anneal to dsDNA and re-signal danger via DNA sensor molecules. A recent paper highlighted a parallel phenomenon concerning ADAR1 editing of dsRNA. Edited molecules were thermodynamically less stable due to lower stacking energy of inosine:thymine pairs—inosine is the product of adenine deamination—and failed to trigger dsRNA sensors (42).

There could be two steps in the catabolism of cytoplasmic ssDNA. A3C, A3F and A3G, which can edit cymtDNA, are expressed in most cells (1,4) and presumably function as constitutive catabolic enzymes. By contrast, A3A (nucleo-cytoplasmic) is massively upregulated by IFNα/β as is A3G (cytoplasmic) albeit to a lesser extent (4,30–32).

When THP-1 cells are triggered by high levels of cytoplasmic DNA, cymtDNA is more edited (Figure 2B and C).

The findings tie in well with the massive egress of mtDNA to the cytosol resulting from a mitochondrial gene lesions or stress following herpesvirus infection (20). Here, the signaling pathway was the DNA sensor cGAS that promoted STING-IRF3-dependent signaling resulting in IFN production. The difference here is that finding pertains to the mouse, which unusually for mammals, does not encode an *A3A* ortholog (43). Although different DNA sensors probably overlap and converge on induction of IFN and a vast array of downstream effector molecules (44) catabolism of the DNA agonist in the mouse may proceed by a different mechanism for we were unable to detect cytosine deaminated mtDNA in mouse tissues (4).

There is a price to pay. Cancer genomes are characterized by tens of thousands to more than a hundred thousand CG→TA transitions, frequently in the tell-tale 5′TpC signature, deamination of 5-methylcytosine residues and large numbers of DNA rearrangements (10,12,34,45–48). The A3A DNA mutator enzyme can reproduce these three mutational hallmarks experimentally (34,37). The link between A3A and cancer has been established epidemiologically (9,10,47,49,50). While both A3A and A3B contribute to mutation of chromosomal DNA (47,51–54), from an experimental setting, A3A is the more active of the two enzymes, A3B activity being greatly attenuated (6,8,9). The major difference is that A3A is massively upregulated by IFNα in hematopoietic cells while A3B is not (4,30–32) and the emergence of cancer on a background of chronic inflammation is well established (55).

Chronic inflammation, autoimmune diseases such as systemic lupus erythematosus and interferonopathies are associated with an increased risk for cancer. All show type I interferon signatures of which A3A is a part. While a powerful catabolic enzyme in the cytoplasm, A3A can locate to the nucleus and mutate nuclear DNA setting up mutation/selection competition between somatically edited cells. Through the interferon paracrine effect, bystander cells too could undergo somatic mutation. It would be interesting to explore A3A-mediated genotoxic damage in other inflammatory pathologies such as diabetes, atherosclerosis and perhaps even ageing. In conclusion, these findings show that the danger signal triggered by exogenous or endogenous cytosolic DNA encodes a mechanism for catabolism of the DNA agonist. A3A can be seen as anti-inflammatory enzyme.

## SUPPLEMENTARY DATA

Supplementary Data are available at NAR Online.

## FUNDING

Institut Pasteur, Centre National de Recherche Scientifique (CNRS); Institut National du Cancer [S-CR14106 to B.M.]; OSEO [FUI AAP12 to V.C.]; Ligue Nationale contre le Cancer [GB/MA/CD-11283 to M.S.B.]. Funding for open access charge: Institut Pasteur.
*Conflict of interest statement.* None declared.

## REFERENCES

1. Jarmuz,A., Chester,A., Bayliss,J., Gisbourne,J., Dunham,I., Scott,J. and Navaratnam,N. (2002) An anthropoid-specific locus of orphan C to U RNA-editing enzymes on chromosome 22. *Genomics*, **79**, 285–296.
2. Beale,R.C., Petersen-Mahrt,S.K., Watt,I.N., Harris,R.S., Rada,C. and Neuberger,M.S. (2004) Comparison of the differential context-dependence of DNA deamination by APOBEC enzymes: correlation with mutation spectra in vivo. *J. Mol. Biol.*, **337**, 585–596.
3. Bishop,K.N., Holmes,R.K., Sheehy,A.M., Davidson,N.O., Cho,S.J. and Malim,M.H. (2004) Cytidine deamination of retroviral DNA by diverse APOBEC proteins. *Curr. Biol.*, **14**, 1392–1396.
4. Suspène,R., Aynaud,M., Guétard,D., Henry,M., Eckhoff,G., Marchio,A., Pineau,P., Dejean,A., Vartanian,J.P. and Wain-Hobson,S. (2011) Somatic hypermutation of human mitochondrial and nuclear DNA by APOBEC3 cytidine deaminases, a pathway for DNA catabolism. *Proc. Natl. Acad. Sci. U.S.A.*, **108**, 4858–4863.
5. Vartanian,J.P., Henry,M., Marchio,A., Suspène,R., Aynaud,M.M., Guétard,D., Cervantes-Gonzalez,M., Battiston,C., Mazzaferro,V., Pineau,P. *et al.* (2010) Massive APOBEC3 editing of hepatitis B viral DNA in cirrhosis. *PLoS Pathog.*, **6**, e1000928.
6. Caval,V., Suspene,R., Shapira,M., Vartanian,J.P. and Wain-Hobson,S. (2014) A prevalent cancer susceptibility APOBEC3A hybrid allele bearing APOBEC3B 3′UTR enhances chromosomal DNA damage. *Nat. Commun.*, **5**, 5129.
7. Landry,S., Narvaiza,I., Linfesty,D.C. and Weitzman,M.D. (2011) APOBEC3A can activate the DNA damage response and cause cell-cycle arrest. *EMBO Rep.*, **12**, 444–450.
8. Caval,V., Bouzidi,M.S., Suspene,R., Laude,H., Dumargne,M.C., Bashamboo,A., Krey,T., Vartanian,J.P. and Wain-Hobson,S. (2015) Molecular basis of the attenuated phenotype of human APOBEC3B DNA mutator enzyme. *Nucleic Acids Res.*, **43**, 9340–9349.
9. Chan,K., Roberts,S.A., Klimczak,L.J., Sterling,J.F., Saini,N., Malc,E.P., Kim,J., Kwiatkowski,D.J., Fargo,D.C., Mieczkowski,P.A. *et al.* (2015) An APOBEC3A hypermutation signature is distinguishable from the signature of background mutagenesis by APOBEC3B in human cancers. *Nat. Genet.*, **47**, 1067–1072.
10. Alexandrov,L.B., Nik-Zainal,S., Wedge,D.C., Aparicio,S.A., Behjati,S., Biankin,A.V., Bignell,G.R., Bolli,N., Borg,A., Borresen-Dale,A.L. *et al.* (2013) Signatures of mutational processes in human cancer. *Nature*, **500**, 415–421.
11. Burns,M.B., Temiz,N.A. and Harris,R.S. (2013) Evidence for APOBEC3B mutagenesis in multiple human cancers. *Nat. Genet.*, **45**, 977–983.
12. Stephens,P.J., Tarpey,P.S., Davies,H., Van Loo,P., Greenman,C., Wedge,D.C., Nik-Zainal,S., Martin,S., Varela,I., Bignell,G.R. *et al.* (2012) The landscape of cancer genes and mutational processes in breast cancer. *Nature*, **486**, 400–404.
13. Komatsu,A., Nagasaki,K., Fujimori,M., Amano,J. and Miki,Y. (2008) Identification of novel deletion polymorphisms in breast cancer. *Int. J. Oncol.*, **33**, 261–270.
14. Zhang,T., Cai,J., Chang,J., Yu,D., Wu,C., Yan,T., Zhai,K., Bi,X., Zhao,H., Xu,J. *et al.* (2012) Evidence of associations of APOBEC3B gene deletion with susceptibility to persistent HBV infection and hepatocellular carcinoma. *Hum. Mol. Genet.*, **22**, 1262–1269.
15. Nik-Zainal,S., Wedge,D.C., Alexandrov,L.B., Petljak,M., Butler,A.P., Bolli,N., Davies,H.R., Knappskog,S., Martin,S., Papaemmanuil,E. *et al.* (2014) Association of a germline copy number polymorphism of APOBEC3A and APOBEC3B with burden of putative APOBEC-dependent mutations in breast cancer. *Nat. Genet.*, **46**, 487–491.
16. Balkwill,F. and Mantovani,A. (2001) Inflammation and cancer: back to Virchow? *Lancet*, **357**, 539–545.
17. Hemmi,H., Takeuchi,O., Kawai,T., Kaisho,T., Sato,S., Sanjo,H., Matsumoto,M., Hoshino,K., Wagner,H., Takeda,K. *et al.* (2000) A Toll-like receptor recognizes bacterial DNA. *Nature*, **408**, 740–745.
18. Atianand,M.K. and Fitzgerald,K.A. (2013) Molecular basis of DNA recognition in the immune system. *J. Immunol.*, **190**, 1911–1918.
19. Yang,P., An,H., Liu,X., Wen,M., Zheng,Y., Rui,Y. and Cao,X. (2010) The cytosolic nucleic acid sensor LRRFIP1 mediates the production of type I interferon via a beta-catenin-dependent pathway. *Nat. Immunol.*, **11**, 487–494.

20. West,A.P., Khoury-Hanold,W., Staron,M., Tal,M.C., Pineda,C.M., Lang,S.M., Bestwick,M., Duguay,B.A., Raimundo,N., MacDuff,D.A. *et al.* (2015) Mitochondrial DNA stress primes the antiviral innate immune response. *Nature*, **520**, 553–557.
21. Ablasser,A., Bauernfeind,F., Hartmann,G., Latz,E., Fitzgerald,K.A. and Hornung,V. (2009) RIG-I-dependent sensing of poly(dA:dT) through the induction of an RNA polymerase III-transcribed RNA intermediate. *Nat. Immunol.*, **10**, 1065–1072.
22. Chiu,Y.H., Macmillan,J.B. and Chen,Z.J. (2009) RNA polymerase III detects cytosolic DNA and induces type I interferons through the RIG-I pathway. *Cell*, **138**, 576–591.
23. Ishikawa,H., Ma,Z. and Barber,G.N. (2009) STING regulates intracellular DNA-mediated, type I interferon-dependent innate immunity. *Nature*, **461**, 788–792.
24. Zhong,B., Yang,Y., Li,S., Wang,Y.Y., Li,Y., Diao,F., Lei,C., He,X., Zhang,L., Tien,P. *et al.* (2008) The adaptor protein MITA links virus-sensing receptors to IRF3 transcription factor activation. *Immunity*, **29**, 538–550.
25. Fernandes-Alnemri,T., Yu,J.W., Datta,P., Wu,J. and Alnemri,E.S. (2009) AIM2 activates the inflammasome and cell death in response to cytoplasmic DNA. *Nature*, **458**, 509–513.
26. Oka,T., Hikoso,S., Yamaguchi,O., Taneike,M., Takeda,T., Tamai,T., Oyabu,J., Murakawa,T., Nakayama,H., Nishida,K. *et al.* (2012) Mitochondrial DNA that escapes from autophagy causes inflammation and heart failure. *Nature*, **485**, 251–255.
27. Zhang,Q., Raoof,M., Chen,Y., Sumi,Y., Sursal,T., Junger,W., Brohi,K., Itagaki,K. and Hauser,C.J. (2010) Circulating mitochondrial DAMPs cause inflammatory responses to injury. *Nature*, **464**, 104–107.
28. Crow,Y.J., Hayward,B.E., Parmar,R., Robins,P., Leitch,A., Ali,M., Black,D.N., van Bokhoven,H., Brunner,H.G., Hamel,B.C. *et al.* (2006) Mutations in the gene encoding the 3′-5′ DNA exonuclease TREX1 cause Aicardi-Goutieres syndrome at the AGS1 locus. *Nat. Genet.*, **38**, 917–920.
29. Yasutomo,K., Horiuchi,T., Kagami,S., Tsukamoto,H., Hashimura,C., Urushihara,M. and Kuroda,Y. (2001) Mutation of DNASE1 in people with systemic lupus erythematosus. *Nat. Genet.*, **28**, 313–314.
30. Bonvin,M., Achermann,F., Greeve,I., Stroka,D., Keogh,A., Inderbitzin,D., Candinas,D., Sommer,P., Wain-Hobson,S., Vartanian,J.P. *et al.* (2006) Interferon-inducible expression of APOBEC3 editing enzymes in human hepatocytes and inhibition of hepatitis B virus replication. *Hepatology*, **43**, 1364–1374.
31. Stenglein,M.D., Burns,M.B., Li,M., Lengyel,J. and Harris,R.S. (2010) APOBEC3 proteins mediate the clearance of foreign DNA from human cells. *Nat. Struct. Mol. Biol.*, **17**, 222–229.
32. Koning,F.A., Newman,E.N., Kim,E.Y., Kunstman,K.J., Wolinsky,S.M. and Malim,M.H. (2009) Defining APOBEC3 expression patterns in human tissues and hematopoietic cell subsets. *J. Virol.*, **83**, 9474–9485.
33. Suspène,R., Henry,M., Guillot,S., Wain-Hobson,S. and Vartanian,J.P. (2005) Recovery of APOBEC3-edited human immunodeficiency virus G->A hypermutants by differential DNA denaturation PCR. *J. Gen. Virol.*, **86**, 125–129.
34. Suspène,R., Aynaud,M.M., Vartanian,J.P. and Wain-Hobson,S. (2013) Efficient deamination of 5-methylcytidine and 5-substituted cytidine residues in DNA by human APOBEC3A cytidine deaminase. *PLoS One*, **8**, e63461.
35. Refsland,E.W., Stenglein,M.D., Shindo,K., Albin,J.S., Brown,W.L. and Harris,R.S. (2010) Quantitative profiling of the full APOBEC3 mRNA repertoire in lymphocytes and tissues: implications for HIV-1 restriction. *Nucleic Acids Res.*, **38**, 4274–4284.
36. Zarember,K.A. and Godowski,P.J. (2002) Tissue expression of human Toll-like receptors and differential regulation of Toll-like receptor mRNAs in leukocytes in response to microbes, their products, and cytokines. *J. Immunol.*, **168**, 554–561.
37. Mussil,B., Suspène,R., Aynaud,M.M., Gauvrit,A., Vartanian,J.P. and Wain-Hobson,S. (2013) Human APOBEC3A isoforms translocate to the nucleus and induce DNA double strand breaks leading to cell stress and death. *PLoS One*, **8**, e73641.
38. Thielen,B.K., McNevin,J.P., McElrath,M.J., Hunt,B.V., Klein,K.C. and Lingappa,J.R. (2010) Innate immune signaling induces high levels of TC-specific deaminase activity in primary monocyte-derived cells through expression of APOBEC3A isoforms. *J. Biol. Chem.*, **285**, 27753–27766.
39. Greagg,M.A., Fogg,M.J., Panayotou,G., Evans,S.J., Connolly,B.A. and Pearl,L.H. (1999) A read-ahead function in archaeal DNA polymerases detects promutagenic template-strand uracil. *Proc. Natl. Acad. Sci. U.S.A.*, **96**, 9045–9050.
40. Wu,L., Pan,J., Thoroddsen,V., Wysong,D.R., Blackman,R.K., Bulawa,C.E., Gould,A.E., Ocain,T.D., Dick,L.R., Errada,P. *et al.* (2003) Novel small-molecule inhibitors of RNA polymerase III. *Eukaryot. Cell*, **2**, 256–264.
41. West,A.P., Shadel,G.S. and Ghosh,S. (2011) Mitochondria in innate immune responses. *Nat. Rev. Immunol.*, **11**, 389–402.
42. Liddicoat,B.J., Piskol,R., Chalk,A.M., Ramaswami,G., Higuchi,M., Hartner,J.C., Li,J.B., Seeburg,P.H. and Walkley,C.R. (2015) RNA editing by ADAR1 prevents MDA5 sensing of endogenous dsRNA as nonself. *Science*, **349**, 1115–1120.
43. Caval,V., Suspene,R., Vartanian,J.P. and Wain-Hobson,S. (2014) Orthologous mammalian APOBEC3A cytidine deaminases hypermutate nuclear DNA. *Mol. Biol. Evol.*, **31**, 330–340.
44. Schoggins,J.W., Wilson,S.J., Panis,M., Murphy,M.Y., Jones,C.T., Bieniasz,P. and Rice,C.M. (2011) A diverse range of gene products are effectors of the type I interferon antiviral response. *Nature*, **472**, 481–485.
45. Denissenko,M.F., Chen,J.X., Tang,M.S. and Pfeifer,G.P. (1997) Cytosine methylation determines hot spots of DNA damage in the human P53 gene. *Proc. Natl. Acad. Sci. U.S.A.*, **94**, 3893–3898.
46. Greenman,C., Stephens,P., Smith,R., Dalgliesh,G.L., Hunter,C., Bignell,G., Davies,H., Teague,J., Butler,A., Stevens,C. *et al.* (2007) Patterns of somatic mutation in human cancer genomes. *Nature*, **446**, 153–158.
47. Nik-Zainal,S., Alexandrov,L.B., Wedge,D.C., Van Loo,P., Greenman,C.D., Raine,K., Jones,D., Hinton,J., Marshall,J., Stebbings,L.A. *et al.* (2012) Mutational processes molding the genomes of 21 breast cancers. *Cell*, **149**, 979–993.
48. Carpenter,M.A., Li,M., Rathore,A., Lackey,L., Law,E.K., Land,A.M., Leonard,B., Shandilya,S.M., Bohn,M.F., Schiffer,C.A. *et al.* (2012) Methylcytosine and normal cytosine deamination by the foreign DNA restriction enzyme APOBEC3A. *J. Biol. Chem.*, **287**, 34801–34808.
49. Roberts,S.A., Lawrence,M.S., Klimczak,L.J., Grimm,S.A., Fargo,D., Stojanov,P., Kiezun,A., Kryukov,G.V., Carter,S.L., Saksena,G. *et al.* (2013) An APOBEC cytidine deaminase mutagenesis pattern is widespread in human cancers. *Nat. Genet.*, **45**, 970–976.
50. Matsuda,K., Takahashi,A., Middlebrooks,C.D., Obara,W., Nasu,Y., Inoue,K., Tamura,K., Yamasaki,I., Naya,Y., Tanikawa,C. *et al.* (2015) Genome-wide association study identified SNP on 15q24 associated with bladder cancer risk in Japanese population. *Hum. Mol. Genet.*, **24**, 1177–1184.
51. Taylor,B.J., Nik-Zainal,S., Wu,Y.L., Stebbings,L.A., Raine,K., Campbell,P.J., Rada,C., Stratton,M.R. and Neuberger,M.S. (2013) DNA deaminases induce break-associated mutation showers with implication of APOBEC3B and 3A in breast cancer kataegis. *eLife*, **2**, e00534.
52. Burns,M.B., Lackey,L., Carpenter,M.A., Rathore,A., Land,A.M., Leonard,B., Refsland,E.W., Kotandeniya,D., Tretyakova,N., Nikas,J.B. *et al.* (2013) APOBEC3B is an enzymatic source of mutation in breast cancer. *Nature*, **494**, 366–370.
53. Hoopes,J.I., Cortez,L.M., Mertz,T.M., Malc,E.P., Mieczkowski,P.A. and Roberts,S.A. (2016) APOBEC3A and APOBEC3B Preferentially Deaminate the Lagging Strand Template during DNA Replication. *Cell Rep.*, **14**, 1273–1282.
54. Seplyarskiy,V.B., Soldatov,R.A., Popadin,K.Y., Antonarakis,S.E., Bazykin,G.A. and Nikolaev,S.I. (2016) APOBEC-induced mutations in human cancers are strongly enriched on the lagging DNA strand during replication. *Genome Res.*, **26**, 174–182.
55. Mantovani,A., Allavena,P., Sica,A. and Balkwill,F. (2008) Cancer-related inflammation. *Nature*, **454**, 436–444.